THERMOCHEMICAL MODELING FOR MISCIBILITY AND STRUCTURAL STABILITIES OF MIXED SYSTEMS OF CHIRAL DOPANTS AND NEMATIC LIQUID CRYSTAL HOSTS

Morgan Bernard*[2], Ariana A. Coley[2], Jewel Harper[1], Kyung Min Lee[3] and Insu Frank Hahn[†1]

[1]Department of Chemistry and Biochemistry, School of Science, Hampton University, Hampton, VA 23668
[2]Department of Biological Sciences, School of Science, Hampton University, Hampton, VA 23668
[3]Air Force Research Laboratory, Wright-Patterson AFB, OH 45433

Abstract

Several mixing intermolecular systems between chiral dopants and an achiral nematic liquid crystal host were experientially studied and theoretically modeled to calculate and predict the intrinsic thermochemical stabilities of those mixtures better to understand their intermolecular miscibility, structures, and behaviors. The resulting thermochemical Gibbs free energy data of the mixtures with different molar ratios show that better miscibility with the achiral nematic host can be achieved as the chiral dopant concentration decreases in the system. In addition, the newly obtained comparative molecular modeling results reveal the significant thermochemical enthalpy changes of the mixtures, showing a more favorable intermolecular bonding trend toward increasing LC monomer amount mixed with chiral dopants. The modeling results revealed that intermolecular mixture systems containing (R)-configured dopants exhibit right-handed (RH) helical structures, whereas (S)-configured dopant forms a left-handed (LH) helical structure, consistent with experimental observations. This study enables a better understanding of the mixing nature of chiral dopant-achiral nematic liquid crystal hosts, as well as aiding the future development of improved LCs for use in various optical applications.

Introduction

Cholesteric liquid crystalline (CLC) materials, also called chiral nematic LCs, are extensively found in nature.[1] These materials self-assemble into selectively reflective 1D photonic crystals that are highly promising for active optical applications including displays, tunable lasers, optical storage, safety goggles, and energy-conserving windows.[2-6] The first liquid crystals were discovered by accident and were simple ester derivatives (mesogens) from naturally-found cholesterol.[7-8] Since their initial discovery, numerous other intrinsically chiral substances, some natural, some semi-synthetic, and some totally synthetic in origin, have been identified as CLC materials.[9]

In addition to intrinsically chiral substances, the CLC phase can be formed through the addition of chiral dopants into achiral nematic liquid crystal (NLC) hosts to produce a helical superstructure. The handedness of the chiral dopant is transferred to the LC resulting in a right-handed (RH) or left-handed (LH) circular rotation of the liquid crystal director (i.e. the average direction of the long molecular axes of the LC) along a helical axis.[2,10]

Achiral NLCs (e.g., 5CB, E7, BL series, TL series, etc.) can be mixed with chiral dopants (e.g., commercially available (R)-1011, (S)-1011, (R)-811, (S)-811, etc.) to produce target compositions resulting in the CLC phase. As is the case of the nematic host molecules, the dopants themselves can be natural, semi-synthetic, or synthetic in origin. The resulting physical properties of a CLC mixture are dependent on the specific identities of hosts and dopants as well as their ratio in the mixture. An example of common chiral dopants and LCs are shown in Figure 1. The

molecular chirality from the chiral dopant compound is transferred to the bulk nematic host forming a helical structure of liquid crystal molecules with left- or right-handed handedness depending on the chiral interactions.[8] The resulting CLC structure is characterized by the pitch P, which is the length of 360° rotation of the director along the helical axis. The pitch of CLC is determined by the ratio of chiral dopant to nematic host in the mixture.[8] The resulting CLC with a helical superstructure exhibits a circularly polarized selective reflection,[2,10] with the center of the reflection notch (λ_0) expressed as

$$\lambda_0 = n_{avg} \times P \qquad (1)$$

where $n_{avg} = \frac{(2n_o + n_e)}{3}$ is the average refractive index of the LC and n_o and n_e are the ordinary and extraordinary refractive indices, respectively. The bandwidth of the reflection band in a CLC is a simple product of the birefringence of the nematic liquid crystal
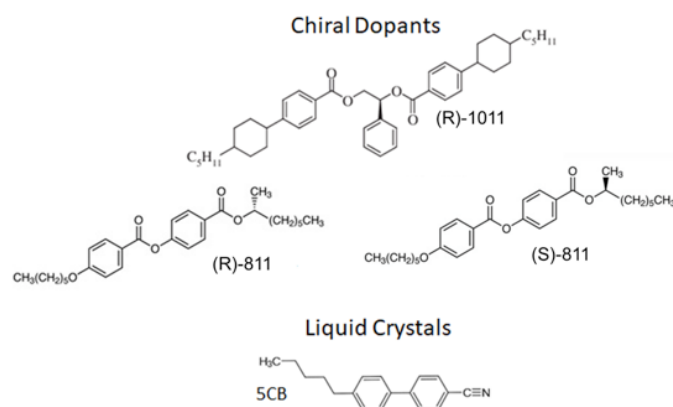

Figure 1. Chemical structures of materials used in this study.

host and the cholesteric pitch length,

$$\Delta\lambda = \Delta n \times P \qquad (2)$$

where $\Delta n = n_e - n_o$ is the birefringence. The bandwidth of a CLC is typically in the range of 50–100 nm in the visible wavelength of the electromagnetic spectrum.

CLCs are prepared by the addition of chiral dopants to achiral NLC hosts to produce a helical superstructure. The miscibility between the chiral dopant and the nematic host is critical, especially for preparing short-pitch CLCs. In many cases, newly synthesized chiral dopants are not highly compatible with the nematic host LCs and phase separation is observed at high chiral dopant concentrations. Hence, it is beneficial to study the miscibility and thermochemical stability information of these mixtures. In this study, we first conducted an experimental study of several mixed intermolecular systems between chiral dopants and NLCs and then theoretically modeled them to calculate and predict the intrinsic thermochemical stability of those mixtures to further determine their intermolecular miscibility, structure and behavior.

Experimental Methods

Preparation of cells and cholesteric liquid crystal samples.
Alignment cells were prepared from ITO-coated glass slides (Colorado Concepts). The glass substrates were cleansed in acetone and methanol, and treated with air plasma for 30 s. The substrates were spin-coated with a polyimide solution (PI2551, HD Microsystems) and baked at 200°C for 1 hr. The preparation of the polyimide solution is as follows: 8 mL of PI2555 polyimide was first dissolved in 32.5 mL of N-methylpyrrolidone (NMP), and then 9.1 mL of 1-methoxy-2propanol was slowly added to the PI solution. The alignment layers were rubbed with a velvet cloth, and the cell was constructed to ensure a planar alignment condition.The cell gap was controlled by mixing 15 μm thick glass rod spacers into an optical adhesive. Samples were prepared by mixing a chiral dopant ((R)-1011 or (R)-811 from Merck) and a positive $\Delta\varepsilon$ nematic liquid crystal (5CB).

Experimental Setup and Measurements.
Transmission spectra were collected with a fiber optic spectrometer (Ocean Optics Spectrometer). Unpolarized, linearly polarized, left-handed or right-handed circularly polarized light was used as a probe beam.

Theoretical approximations.
The computer processor used for multiple computers was 11th Gen Intel® Core ™ i7-1165G7 CPU @ 2.8GHz 1.69 GHz, installed (memory) Ram used 16.00GB. The system type was a 64-bit operating system. Software programs used were ChemOffice® Ultra version 21.0.0.28 (PerkinElmer, MA, U.S.A), MOPAC (Molecular Orbital Package) and Gaussian 03W version 6.1 (Gaussian, Inc., CT, USA) for molecular modeling and thermochemical calculations. The molecular orbital package (MOPAC 2016) and Gaussian (G03W and G16W) interfaces for semi-empirical (PM3, PM6, and PM7) and higher-level DFT calculations (6-31G or 6-311G** basis set) were tested to find an optimum theoretical computation method for the targeted mixture molecules in the gas phase at 298.15 °K and 1.0000 atm,

considering complicated mixture molecule geometries and their atom limits for each calculation method. The semi-empirical theory for the MOPAC and Gaussian theoretical computations was the EF (Eigenvector Following) optimizer, no solvent (gas), and default Hartree-Fock closed-shell (restricted) wave function, minimum RMS (0.1000), and shift virtual M.O. energy level of 80. PM3 was used to compute thermochemical data for the stability and miscibility information of the tested mixture molecules. Hess's law and related fundamental thermochemical theories were used to obtain the thermochemical information ($\Delta H°_f$, $\Delta H°_{mixture}$, $\Delta S°_{mixture}$, and $\Delta G°_{mixture}$) for all tested molecules. All molecular modeling data was treated with the chemometrics process.

Results and Discussion

Figure 2 shows the experimental transmission spectra of two CLC mixtures containing different chiral dopants ((R)-1011 and (R)-811) at varying concentrations. As the chiral dopant concentration increases, the reflection band of CLC shifts to a lower wavelength range due to a reduction in the helical pitch. As stated previously, λ_0 is influenced by the helical pitch, which is inversely proportional to the concentration of the chiral dopant. Each chiral dopant has a different ability to twist nematic LCs, which is defined as helical twisting power (HTP). HTP is defined as

$$HTP = \frac{1}{(P \times c \times \beta)} \qquad (3)$$

where P is the pitch, c is the weight concentration of the chiral dopant, and β is the enantiomeric purity of the chiral dopant.[11-13] The enantiomeric purity (β) is generally 1 as the chiral dopants are purified to remove the undesired enantiomer. It should be noted that HTP values are dependent on the LC host, and the values can change slightly across different LC systems. The HTPs of (R)-1011 and (R)-811 in 5CB are ~35 μm⁻¹ and ~13 μm⁻¹, respectively.[14] In general, chiral dopants with a high HTP have lower solubility in the LC host because the interaction between the chiral dopants is stronger than the interaction between the chiral dopant and the LC.[13] For example, (R)-1011 can be dissolved in the 5CB up to a concentration of at least 7.45 wt%, but undergoes a phase separation and crystallizes around 6.60 wt%. Such crystallization not only destroys the liquid crystalline properties of the system but also makes it incompatible with any kind of optical application. However, low HTP (R)-811 forms a stable cholesteric phase up to 14.6 wt% in the LC 5CB medium. At higher concentrations, however, (R)-811 crystallization was observed like samples with high concentrations of (R)-1011.
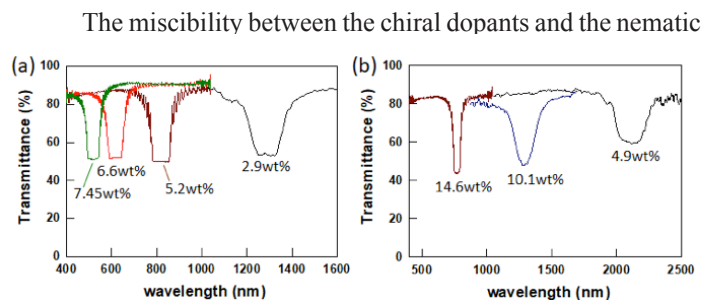
The miscibility between the chiral dopants and the nematic

Figure 2. Transmission spectra of CLC mixtures with various chiral dopant concentrations. (a) 2.9 wt%, 5.2 wt%, 6.6 wt% and 7.5 wt% (R)-1011 dissolved in 5CB and (b) 4.9 wt%, 10.1 wt% and 14.6 wt% (R)-811 dissolved in 5CB.

host is critical, especially for short-pitch CLCs which require a large percentage of dopant to be added. Hence, it is beneficial to study these mixtures' miscibility and thermochemical stability information. In this study, several systems comprised of chiral dopants ((R)-1011, (R)-811 and (S)-811) and an achiral NLC (5CB) were theoretically modeled to calculate and predict the intrinsic thermochemical stabilities of the mixtures to better understand the intermolecular miscibility, helical structures, and helical rotation behaviors. For this theoretical modeling, quantum chemical 3-D molecular modeling techniques including semi-empirical simulations and Density functional theory (DFT) calculations were explored for their theoretical thermochemical properties.[15-17] Based on thermochemical enthalpy, entropy, and Gibb's free energy data showing the mixture's stability and miscibility,[17-19] the resulting computational chemistry data of those mixtures were compared to better understand the interplay between chiral dopants and achiral NLC hosts. This allows us to better understand the mixing nature of chiral dopant-achiral nematic liquid crystal host, as well as develop optimal CLCs and LCs for use in a variety of optical applications.

The 3D molecular models of chiral dopants (R)-1011, (R)-811, and (S)-811, as well as nematic host 5CB, were optimized for bond lengths and angles using semi-empirical methods. The optimized bond lengths and angles were then used to model one molecule of each chiral dopant with a varying number of 5CB molecules. Gaussian Z-matrix and Cartesian functions were used to create the models for (R)-1011-5CB (1:3 molar ratio). Figure 3 shows the modeling results of (R)-1011-5CB with a 1:3 molar ratio and (R)-811-5CB with 1:5 molar ratio. Figures S1 and S2 summarize the modeling results for (R)-1011-5CB with molar ratios of 1:1 and 1:2 and (R)-811-5CB with molar ratios of 1:1 and 1:3. All samples show right-handed helical structures. In addition, the helical structure and handedness of the left-handed chiral dopant (S)-811 and 5CB mixture were modeled with the same theoretical method for comparison with the right-handed (R)-811-5CB mixture (Figure 4). This sample (S)-811-5CB has a left-handed helical structure. Figure 5 shows the transmission spectra of CLC mixtures of (R)-811-5CB and (S)-811-5CB (1:4 wt. ratio) obtained at 15 °C. Since the CLC mixture is isotropic at room temperature
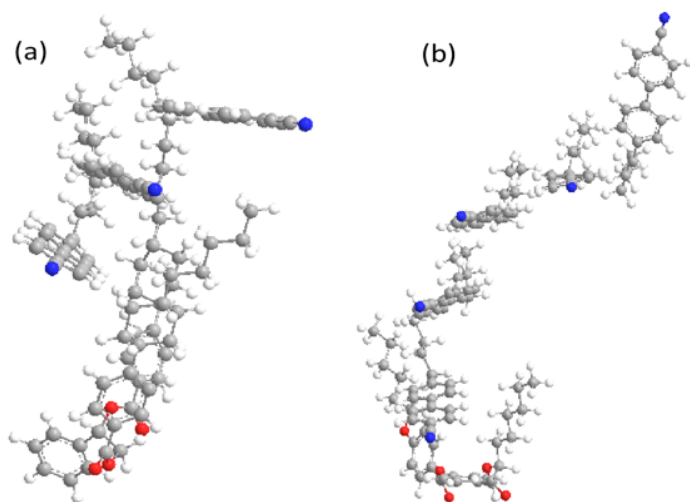
(23~25 °C), the reflection notch (cholesteric phase) is obtained at temperatures slightly below room temperature. These CLCs show selective reflection of circularly polarized light (CPL). When unpolarized light is used as the probe beam, both RH CLC and LH CLC mixtures exhibit 50% reflection. However, when a right-handed or left-handed CPL is used as the probe beam, different CLCs show different responses. In Figure 5(a), RH CLC shows very low transmittance at a wavelength of ~690 nm when using RH circularly polarized light (RH CPL), whereas no distinct peak is observed when using LH CPL as the probe beam. Conversely, the LH CLC mixture exhibits very low transmittance at a wavelength of ~690 nm when the LH CPL is used as the probe beam. This indicates that the optical response of CLCs with different hands is different.

After testing Semiempirical (PM3, PM6, and PM7) and DFT calculation methods to find an optimum and consistent calculation method for all tested LC mixtures, it was found that PM3 semiempirical computation theory was the best working method to obtain optimum structures and thermochemical data for the tested mixture molecules.[17-19] However, PM6, PM7, and DFT methods did not work due to the tested molecule's atomic sizes with utilized computer hardware. Perhaps further future studies need to be done with high performance computing. Since no phase changes occur
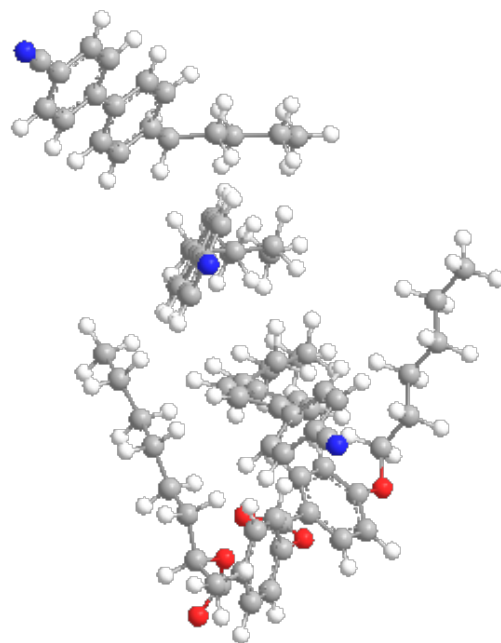

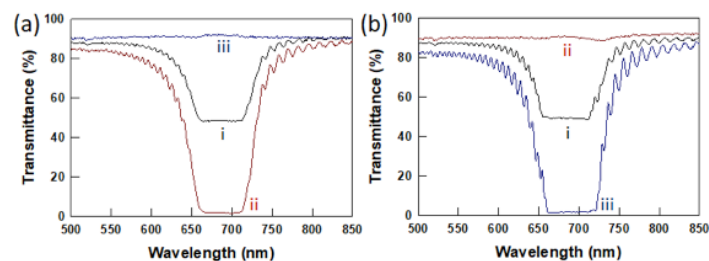**Figure 4.** An optimized molecular model structure (1:3 molar ratio) of (S)-811-5CB.

Figure 5. Transmission spectra of CLC mixtures at 15 °C with 20wt% (a) (R)-811 and (b) (S)-811 in 5CB under various probe beams: i – unpolarized light, ii – RH circularly polarized light (RH CPL), and iii – LH CPL. These mixtures are isotropic at room temperature (23-25 °C). A cell with a thickness of 15 µm was used.

Figure 3. Representative optimized molecular model structures (1:3 and 1:5 molar ratios) of (R)-1011-5CB (a) and (R)-811-5CB (b), respectively. The red symbols in chiral dopants and blue symbols in 5CB represent oxygen and nitrogen, respectively.

over the temperature changes used in the theoretical calculations, gas phase approximation at 298.15 °K and 1.0000 atm was applied to those mixture systems. To assess thermochemical stability and miscibility, changes of thermochemical enthalpy, entropy, and Gibbs free energy were estimated.[20-22] For this study, the heat of formations ($\Delta H°_f$) values for (R)-1011, (R)-811, (S)-811 and (5)-CB were first acquired to support thermochemical approximations regarding structural stability and miscibility among the mixtures of RH chiral dopants and 5CB, as shown in Table 1. Similar heat of formation values are observed for (R)-811 and (S)-811. The heat of formation data provided an initial assessment of the molecules' stability, showing that (R)-811 and (S)-811 exhibited the highest stability among the tested structures, followed by (R)-1011, with 5CB displaying the least stability.

First, thermochemical data were obtained for mixtures of (R)-1011 and 5CB with various molar ratios. The thermochemical enthalpy ($\Delta H°$) changes of the (R)-1011 and 5CB mixtures show more favorable intermolecular bonding patterns with increasing LC concentration (lower chiral dopant concentration), as shown in Table 2. Also, the resulting thermochemical Gibbs free energy ($\Delta G°$) and entropy ($\Delta S°$) data of the mixtures indicate that enhanced miscibility can be achieved at higher LC concentrations. Lastly, these mixtures have a right-handed (RH) helical structure (Figure 3) as observed in our experiments (Figure 5).

The thermochemical data obtained for the intermolecular mixtures between (R)-811-5CB and (S)-811-5CB with different molar ratios are summarized in Table 3. Observing the exothermic reaction enthalpy due to regular intermolecular bonding and geometric polarity, it is clear that the interaction between the mixed components is favorable. The mixture systems can be deduced as ideal solutions by following typical thermochemical reaction pathways. Also, low entropies obtained indicate that as predicted, there are no phase separations. The CLC mixture systems of (R)-811/(S)-811 and 5 CB have fewer atoms than (R)-1011-5CB

systems but follow the same stability and miscibility trends as described above. Therefore, a more stable system with enhanced chiral dopant miscibility can be achieved at higher achiral nematic LC concentrations or lower chiral dopant concentrations. Similar entropy values are obtained for the (R)-811-5CB and (S)-811-5CB mixtures.

Introducing a chiral molecule into an achiral liquid crystal host transfers the chirality of the chiral molecule to the entire system. This makes the liquid crystal into a right- or left-handed helical structure depending on the chiral dopant added, and each chiral molecule has the ability to induce various degrees of twist in the LC host. That is, the achiral nematic liquid crystal has the same chiral conformations twisted with the same helical twist as the chiral dopant.[23-26] Figures 3, 4 and Figures S1 and S2 illustrate the results of our testing, where we investigated the chiral handedness of (R)-811 and (S)-811 compounds in the 5CB host. The findings demonstrated that (R)-811 induces the right-handed (RH) helical structure of CLC, whereas (S)-811 exhibits the left-handed (LH) helical structure of CLC, which is consistent with the experimental results.

Conclusions

The newly obtained comparative modeling results and their thermochemical pathway data show that greater chiral dopant

Table 1. Heat of formations ($\Delta H°_f$) obtained for (R)-1011, (R)-811, (S)-811 and 5CB.

Heat of formation[1]	**(R)-1011**	**(R)-811**	**(S)-811**	**5CB**
$\Delta H°_f$ (kcal/mol)	-180.7674 ± 0.0006	-205.9737 ± 0.0001	-206.3526± 0.0001	52.2725 ± 0.0001

[1]for compounds in gas phase at 298.15 °K and 1.0000 atm.

Table 2. Thermochemical data obtained for the intermolecular mixtures between (R)-1011 and 5CB having different molar ratios.

Mixture molar ratios ((R)-1011 vs. 5CB)	$\Delta H°$ (kcal/mol) [1]	$\Delta S°$ (kcal/mol · K) [1]	$\Delta G°$ (kcal/mol) [1]
1:1	-8.0910 ± 0.0006	0.3964 ± 0.0001	-126.2057 ± 0.0006
1:2	-19.7144 ± 0.0006	0.4777 ± 0.0001	-162.0666± 0.0006
1:3	-27.7234 ± 0.0006	0.5503 ± 0.0001	-191.7274 ± 0.0006

[1]for mixtures in gas phase at 298.15 °K and 1.0000 atm.

Table 3. Thermochemical data obtained for the intermolecular mixtures between (R)-811/(S)-811 and 5CB having different molar ratios.

Mixture molar ratios ((R)-811/(S)-811[2] vs. 5CB)	$\Delta H°$ (kcal/mol) [1]	$\Delta S°$ (kcal/mol · K) [1]	$\Delta G°$ (kcal/mol) [1]
1:1	-10.9186 ± 0.0001	0.3212 ± 0.0001	-106.6356 ± 0.0001
1:3	-21.8776 ± 0.0001	0.5480 ± 0.0001	-185.1932 ± 0.0001
1:5	-35.6825 ± 0.0001	0.7217 ± 0.0001	-250.7616 ± 0.0001
1:3[2]	-26.8241 ± 0.0001	0.5107 ± 0.0001	-179.0165 ± 0.0001

[1]for mixtures in gas phase at 298.15 °K and 1.0000 atm. [2]for (S)-811 and 5CB
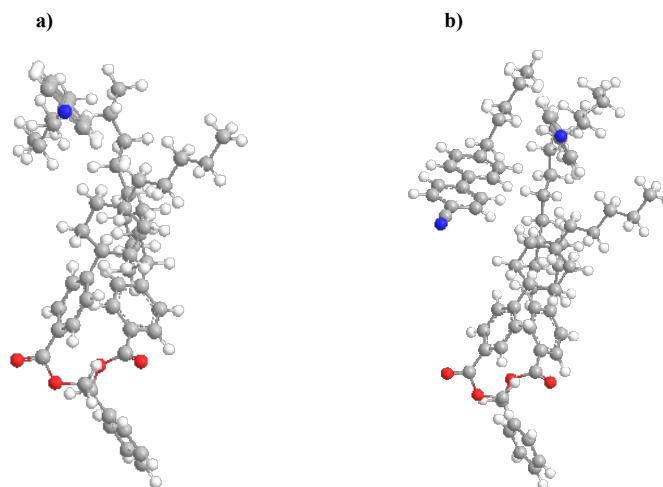

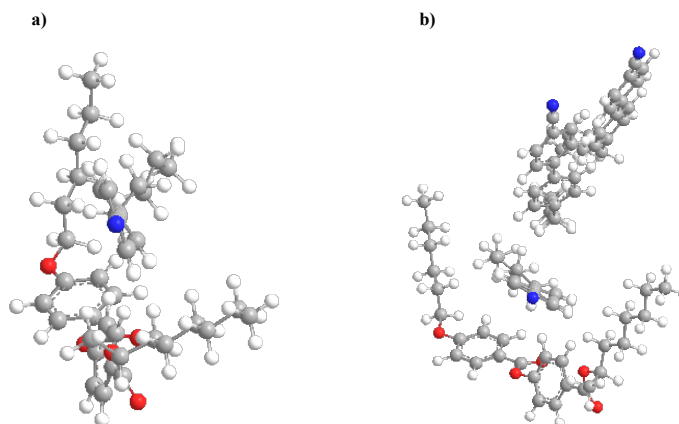**Figure S1**. (a) 1:1 and (b) 1:2 (R)-1011-5CB

Figure S2. (a) 1:1 and (b) 1:3 (R)-811-5CB

stability and miscibility can be achieved by lowering ΔG° and ΔH° by increasing the LC concentration. The modeling results also determined that the intermolecular mixture systems containing (R)-1011 and (R)-811 have RH helical structures, while (S)-811 has a LH helical structure, as observed experimentally. Although current modeling methods have limitations on the number of atoms of chiral dopants and liquid crystals, these results will contribute to a better understanding of the mixing nature of chiral dopant-achiral nematic LC host systems. A better understanding of cholesteric LC systems will help develop LCs for use in a variety of optical applications including displays, tunable lasers, optical storage devices, safety goggles and energy saving windows.

Acknowledgement

References

1. Mitov, M., Cholesteric liquid crystals in living matter. *Soft Matter* **2017,** 13, 4176–4209.
2. Wu, S. T.; Yang, D.-K., *Reflective Liquid Crystal Displays*. Wiley: West Sussex, UK, 2001.
3. Coles, H.; Morris, S., Liquid-crystal lasers. *Nat. Photonics* **2010,** 4, 676-685.
4. Haas, W.; Adams, J.; Dir, G., Optical storage effects in liquid crystals. *Chem. Phys. Lett.* **1972,** 14, 95-97.
5. Tamaoki, N., Cholesteric Liquid Crystals for Color Information Technology. *Adv. Mater.* **2001,** 13, 1135-1147.
6. Addington, M.; Schodek, D., *Smart Materials and Technologies for the Architecture and Design Professions*. Architectural Press: Oxford, 2005.
7. Reinitzer, F., eiträge zur kenntniss des cholesterins. *Monatsh. Chem. Verw. Teile. Anderer. Wiss.* **1888,** 9, 421–441.
8. Guimarães, V. G.; Svanidze, A.; Guo, T.; Nepal, P.; Twieg, R. J.; Palffy-Muhoray, P.; Yokoyama, H., Synthesis and Characterization of Novel Bio-Chiral Dopants Obtained from Bio-Betulin Produced by a Fermentation Process. *Crystals* **2021,** 11, 785.
9. Taugerbeck, A.; Booth, C. J., Design and Synthesis of Chiral Nematic Liquid Crystals. In *Handbook of Liquid Crystals*, Wiley: Hoboken, NJ, USA, 2014; Vol. 3.
10. Kitzerow, H. S.; Bahr, C., *Chirality in Liquid Crystals*. Springer-Verlag: New York, 2001.
11. Wilson, M. R.; Earl, D. J., Calculating the helical twisting power of chiral dopants. *J. Mater. Chem.* **2001,** 11, 2672-2677.
12. Cook, M. J.; Wilson, M. R., Calculation of helical twisting power for liquid crystal chiral dopants. *J. Chem. Phys.* **2000,** 112, 1560-1564.
13. Duda, Ł.; Czajkowski M.; Potaniec, B.; Vaňkátová, P., Helical twisting power and compatibility in twisted nematic phase of new chiral liquid crystalline dopants with various liquid crystalline matrices. *Liq. Cryst.* **2019,** 46, 1769-1779.
14. Lee, K. M.; Tohgha, U.; Bunning, T. J.; McConney, M. E.; Godman, N. P., Effect of Amorphous Crosslinker on Phase Behavior and Electro-Optic Response of Polymer-Stabilized Blue Phase Liquid Crystals. *Nanomaterials* **2022,** 12, 48.
15. Thiel, W., Semiempirical quantum-chemical methods. *Wiley Interdiscip. Rev. Comput. Mol. Sci.* **2013,** 4, 145-157.
16. Manzoor, A.; Pandey, S.; Chakraborty, D.; Phillpot, S. R.; Aidhy, D. S., Entropy contributions to phase stability in binary random solid solutions. *npj Comput. Mater.* **2018,** 4, 47.
17. Yoshizawa, A., Liquid-Crystalline Supermolecules Inducing Layer Fluctuations: From Hierarchical to Dissipative Structures. *Crystals* **2024**, *14*, 681. https://doi.org/10.3390/cryst14080681.
18. Yu, H.; Ikeda T., Photocontrollable Liquid-Crystalline Actuators. Adv. Mater. **2011**, 23,2149–2180. DOI: 10.1002/adma.201100131.
19. Stewart JJ. Optimization of parameters for semiempirical methods V: modification of NDDO approximations and application to 70 elements. J Mol Model. **2007** Dec;13(12):1173-213. doi: 10.1007/s00894-007-0233-4. Epub 2007 Sep 9. PMID: 17828561; PMCID: PMC2039871
20. Hao, X.; Liu, J.; Luo, H.; Han, Y.; Hu, W.; Liu, J.; Li, J.; He, X., Crystal Structure Optimization and Gibbs Free Energy Comparison of Five Sulfathiazole Polymorphs by the Embedded Fragment QM Method at the DFT Level. *Crystals* **2019,** 9, 256.
21. Li, J. J.; Sode, O.; Voth, G. A.; Hirata, S., A solid-solid phase transition in carbon dioxide at high pressures and intermediate temperatures. *Nat. Commun.* **2013,** 4, 141–155.
22. Li, J. J.; Sode, O.; Hirata, S., Second-Order Many-Body Perturbation Study on Thermal Expansion of Solid Carbon Dioxide. *J. Chem. Theory Comput.* **2015,** 11, 224–229.
23. Earl, D. J.; Wilson, M. R., Predictions of moledular chirality and helical twaisitng powers: A theoretical study. *J. Chem. Phys.* **2003,** 119, 215.
24. M. C. W. van Boxtel; R. H. C. Janssen; C. W. M. Bastiaansen; D. J. Broer, *J. Appl. Phys.* **2001,** 89, 838.
25. M. Schadt; H. Seiberle; Schuster, A., *Nature* **1996,** 381, 6579.
26. P. van de Witte; E. E. Neteboom; M. Brehmer; Lub, J., *J. Appl. Phys.* **1999,** 85, 7517.